

A Family of New Glutarate Compounds: Synthesis, Crystal Structures of: $\text{Co}(\text{H}_2\text{O})_5\text{L}$ (**1**), $\text{Na}_2[\text{CoL}_2]$ (**2**), $\text{Na}_2[\text{L}(\text{H}_2\text{L})_{4/2}]$ (**3**), $\{[\text{Co}_3(\text{H}_2\text{O})_6\text{L}_2](\text{HL})_2\} \cdot 4\text{H}_2\text{O}$ (**4**), $\{[\text{Co}_3(\text{H}_2\text{O})_6\text{L}_2](\text{HL})_2\} \cdot 10\text{H}_2\text{O}$ (**5**), $\{[\text{Co}_3(\text{H}_2\text{O})_6\text{L}_2]\text{L}_{2/2}\} \cdot 4\text{H}_2\text{O}$ (**6**), and $\text{Na}_2\{[\text{Co}_3(\text{H}_2\text{O})_2]\text{L}_{8/2}\} \cdot 6\text{H}_2\text{O}$ (**7**), and Magnetic Properties of **1** and **2** with $\text{H}_2\text{L} = \text{HOOC}-(\text{CH}_2)_3-\text{COOH}$

Yue-Qing Zheng,* Jian-Li Lin, Wei Xu, Hong-Zhen Xie, Jie Sun, and Xian-Wen Wang

Institute of Solid Materials Chemistry, State Key Laboratory Base of Novel Functional Materials & Preparation Science, Faculty of Materials Science & Chemical Engineering, Ningbo University, Ningbo 315211, P.R. China

Received June 7, 2008

Seven new glutaric acid complexes, $\text{Co}(\text{H}_2\text{O})_5\text{L}$ **1**, $\text{Na}_2[\text{CoL}_2]$ **2**, $\text{Na}_2[\text{L}(\text{H}_2\text{L})_{4/2}]$ **3**, $\{[\text{Co}_3(\text{H}_2\text{O})_6\text{L}_2](\text{HL})_2\} \cdot 4\text{H}_2\text{O}$ **4**, $\{[\text{Co}_3(\text{H}_2\text{O})_6\text{L}_2](\text{HL})_2\} \cdot 10\text{H}_2\text{O}$ **5**, $\{[\text{Co}_3(\text{H}_2\text{O})_6\text{L}_2]\text{L}_{2/2}\} \cdot 4\text{H}_2\text{O}$ **6**, and $\text{Na}_2\{[\text{Co}_3(\text{H}_2\text{O})_2]\text{L}_{8/2}\} \cdot 6\text{H}_2\text{O}$ **7** were obtained and characterized by single-crystal X-ray diffraction methods along with elemental analyses, IR spectroscopic and magnetic measurements (for **1** and **2**). The $[\text{Co}(\text{H}_2\text{O})_5\text{L}]$ complex molecules in **1** are assembled into a three-dimensional supramolecular architecture based on intermolecular hydrogen bonds. Compound **2** consists of the Na^+ cations and the necklace-like glutarato doubly bridged $[\text{CoL}_2]^{2-}$ anionic chains, and **3** is composed of the Na^+ cations and the anionic hydrogen bonded ladder-like $[\text{L}(\text{H}_2\text{L})_{4/2}]^{2-}$ anionic chains. The trinuclear $\{[\text{Co}_3(\text{H}_2\text{O})_6\text{L}_2](\text{HL})_2\}$ complex molecules with edge-shared linear trioctahedral $[\text{Co}_3(\text{H}_2\text{O})_6\text{L}_2]^{2+}$ cluster cores in **4** and **5** are hydrogen bonded into two-dimensional (2D) networks. The edge-shared linear trioctahedral $[\text{Co}_3(\text{H}_2\text{O})_6\text{L}_2]^{2+}$ cluster cores in **6** are bridged by glutarato ligands to generate one-dimensional (1D) chains, which are then assembled via interchain hydrogen bonds into 2D supramolecular networks. The corner-shared linear $[\text{Co}_3\text{O}_{16}]$ trioctahedra in **7** are quaternate bridged by glutarato ligands to form 1D band-like anionic $\{[\text{Co}_3(\text{H}_2\text{O})_2]\text{L}_{8/2}\}^{2+}$ chains, which are assembled via interchain hydrogen bonds into 2D layers, and between them are sandwiched the Na^+ cations. The magnetic behaviors of **1** and **2** obey the Curie–Weiss law with $\chi_m = C/(T - \Theta)$ with the Curie constant $C = 3.012(8) \text{ cm}^3 \cdot \text{mol}^{-1} \cdot \text{K}$ and the Weiss constant $\Theta = -9.4(7) \text{ K}$ for **1**, as well as $C = 2.40(1) \text{ cm}^3 \cdot \text{mol}^{-1} \cdot \text{K}$ and $\Theta = -2.10(5) \text{ K}$ for **2**, indicating weak antiferromagnetic interactions between the $\text{Co}(\text{II})$ ions.

Introduction

Over the past decades, rational design and synthesis of metal-organic coordination polymers has become one of the most active areas of chemical research and materials science, owing not only to their intriguing structural topologies but also their potential applications in optics, electronics, catalysis, medicine, host–guest chemistry, ion exchange, gas storage, photoluminescence, and the molecular-based magnetic materials.¹ The judicious choices of special inorganic and organic building blocks are the key steps for designing such materials with desired structural motifs and properties.²

Among the organic building blocks used, carboxylic acids have been widely employed for this purpose.³ For example, the aromatic polycarboxylic acid ligands such as benzene-1,4-dicarboxylic acid and benzene-1,3,5-tricarboxylic acid are good candidates for the construction of open metal organic frameworks (MOFs).⁴ In contrast to the rigid aromatic polycarboxylic acid ligands, aliphatic α,ω -dicarboxylic acids are of special interest because of their versatile coordination modes and conformational flexibility.⁵ The most remarkable contributions to the construction of coordination polymers with α,ω -dicarboxylic acid ligands have been made by Férey and co-workers, who evidenced that hydrothermal self-assembly of $\text{Co}(\text{II})$ ions and succinic acid afforded a

* To whom correspondence should be addressed. E-mail: zhengcm@nbu.edu.cn. Fax: +574/87600747.

family of cobalt succinate coordination polymers with markedly different structures, MIL-9, MIL-16, $\text{Co}(\text{H}_2\text{O})_2(\text{C}_4\text{H}_4\text{O}_4)$, and $\text{Co}_6(\text{OH})_2(\text{C}_4\text{H}_4\text{O}_4)_5 \cdot 0.5\text{H}_2\text{O}$ depending on reactant ratios, stoichiometries, and pH values.⁶ Different from the rich members and structural diversity of Co(II) succinate coordination polymers, hydrothermal self-assembly of Co(II) ions and glutaric acid reportedly yielded only a seemingly simple coordination polymer $\text{Co}(\text{C}_3\text{H}_6\text{O}_4)$ with the tetrahedrally coordinated Co(II) centers interlinked by both gauche- and the anti-conformational glutarate ligands into a three-dimensional (3D) structure consisting of infinite Co—CO₂—Co inorganic layers.⁷ The rich coordination chemistry in cobalt succinates stimulates our impetus further to investigate self-assemblies of Co(II) and glutaric acid in aqueous solutions, which enable us to isolate six new cobalt glutarates, $\text{Co}(\text{H}_2\text{O})_5\text{L}$ **1**, $\text{Na}_2[\text{CoL}_2]$ **2**, $\{[\text{Co}_3(\text{H}_2\text{O})_6\text{L}_2](\text{HL})_2\} \cdot 4\text{H}_2\text{O}$ **4**, $\{[\text{Co}_3(\text{H}_2\text{O})_6\text{L}_2](\text{HL})_2\} \cdot 10\text{H}_2\text{O}$ **5**, $\{[\text{Co}_3(\text{H}_2\text{O})_6\text{L}_2]_{\text{L}2/2}\} \cdot 4\text{H}_2\text{O}$ **6**, and $\text{Na}_2\{[\text{Co}_3(\text{H}_2\text{O})_2]_{\text{L}8/2}\} \cdot 6\text{H}_2\text{O}$ **7**, along with a new sodium glutarate $\text{Na}_2[\text{L}(\text{H}_2\text{L})_{4/2}]$ **3** with $\text{H}_2\text{L} = \text{HOOC}-(\text{CH}_2)_3-\text{COOH}$. Here, we wish to report our results about syntheses, crystal structures along with IR spectroscopic and magnetic characterizations (for **1** and **2**).

Experimental Section

Materials. All chemicals of reagent grade were commercially available and used without further purification.

Physical Methods. The C and H microanalyses were performed with a Perkin-Elmer 2400II elemental analyzer. The FT-IR spectra were recorded from KBr pellets in the range 4000–400 cm^{-1} on a Shimadzu FTIR-8900 spectrometer. The magnetic susceptibilities were measured using a SQUID magnetometer (Quantum Design Model MPMS-7) in temperature range $2 \leq T$ (K) ≤ 300 with an applied field of 2000 G. Diamagnetic corrections were estimated from Pascal's constants.⁸

Synthesis of $\text{Co}(\text{H}_2\text{O})_5\text{L}$ **1.** An aqueous solution of glutaric acid (0.132 g, 1.00 mmol) in 10.0 mL of water was neutralized with NaOH (1 M), and then $\text{Co}(\text{ClO}_4)_2 \cdot 6\text{H}_2\text{O}$ (0.365 g, 1.00 mmol) was added under continuous stirring. The mixture was stirred further for 1 h and filtered off. The filtrate was allowed to stand at room temperature and slow evaporation afforded rose-colored block crystals of **1** (yield 95% based on the initial $\text{Co}(\text{ClO}_4)_2 \cdot 6\text{H}_2\text{O}$ input). Anal. Calcd for $\text{C}_5\text{H}_{16}\text{CoO}_9$ (%): C, 21.52; H, 5.78. Found: C, 21.46; H, 5.63. IR data (cm^{-1} , KBr): 3404s, 2958s, 1680m, 1564s, 1541s, 1460m, 1415m, 1355s, 1315w, 1224m, 1161w, 1072w, 860m, 769m, 725m, 675m, 588w.

Synthesis of $\text{Na}_2[\text{CoL}_2]$ **2.** A mixture of $\text{Co}(\text{ClO}_4)_2 \cdot 6\text{H}_2\text{O}$ (0.365 g, 1.00 mmol), glutaric acid (0.132 g, 1.00 mmol), NaOH (0.080 g, 1.00 mmol), 4,4'-bipyridine (0.198 g, 1.00 mmol), and H_2O (23.0 mL) in the mole ratio of approximately 1:1:2:1:131 was sealed in a 25 mL Teflon-lined stainless-steel autoclave, which was heated to 120 °C and kept at this temperature for 120 h, then cooled to room temperature and filtered off. The red filtrate was allowed to stand at room temperature. Slow evaporation for 1 month afforded purple prismatic crystals of **2** (yield: 85% based on the initial $\text{Co}(\text{ClO}_4)_2 \cdot 6\text{H}_2\text{O}$ input). Anal. Calcd for $\text{C}_{10}\text{H}_{12}\text{CoNa}_2\text{O}_8$ (%): C, 32.90; H, 3.31. Found: C, 32.85; H, 3.33. IR data (cm^{-1} , KBr): 2970s, 1623s, 1600s, 1463m, 1434m, 1386s, 1303m, 1253m, 1120w, 1066m, 1029w, 935w, 798w, 682m, 665m, 511w.

Synthesis of $\text{Na}_2[\text{L}(\text{H}_2\text{L})_{4/2}]$ **3, $\{[\text{Co}_3(\text{H}_2\text{O})_6\text{L}_2](\text{HL})_2\} \cdot 4\text{H}_2\text{O}$ **4**, and $\{[\text{Co}_3(\text{H}_2\text{O})_6\text{L}_2](\text{HL})_2\} \cdot 10\text{H}_2\text{O}$ **5**.** A 5.0 mL (1 M) amount of Na_2CO_3 was dropwise added to a stirred aqueous solution of glutaric acid (0.23 g, 1.74 mmol) and $\text{CoCl}_2 \cdot 6\text{H}_2\text{O}$ (0.50 g, 1.72 mmol) in 15.0 mL of H_2O , and the resulting reddish precipitate was filtered off. The filtrate was maintained at room temperature for 24 h, and a small amount of colorless crystals of **3** were grown. The crystals were filtered off, washed with a small amount of ether, then air-dried at about 25 °C, and the filtrate was loaded in a 23 mL Teflon-lined stainless-steel autoclave, which was then heated to 150 °C and kept at constant temperature for 72 h, then cooled to room temperature. The solution was filtered, and the filtrate was allowed to stand at room temperature. Slow evaporation for 2 weeks yielded a mixture of rose-colored crystals of **4** and **5**. Unfortunately, their extreme similarity in color and shape made it impossible to separate them from each other, so that no further effort was dedicated to the optimization of the synthetic procedures.

Synthesis of $\{[\text{Co}_3(\text{H}_2\text{O})_6\text{L}_2]_{\text{L}2/2}\} \cdot 4\text{H}_2\text{O}$ **6, $\text{Na}_2\{[\text{Co}_3(\text{H}_2\text{O})_2]_{\text{L}8/2}\} \cdot 6\text{H}_2\text{O}$ **7**.** A mixture of rose-colored crystals of **6** and **7** were obtained in an analogous procedure described above for **4** and **5** except that 5.0 mL (1 M) of NaOH was used instead of Na_2CO_3 . Because the crystals of **6** and **7** exhibit similar color and habitus, no attempt was made to separate them from each other.

X-ray Crystallography. Suitable single crystals were selected under a polarizing microscope and fixed with epoxy cement on

- (1) (a) Batten, S. R.; Robson, R. *Angew. Chem., Int. Ed.* **1998**, *37*, 1460–1494. (b) Eddaoudi, M.; Moler, D. B.; Li, H. L.; Chen, B. L.; Reineke, T. M.; O'Keeffe, M.; Yaghi, O. M. *Acc. Chem. Res.* **2001**, *34*, 319–330. (c) Zaworotko, M. J. *Chem. Commun.* **2001**, 1–9. (d) Evans, O. R.; Lin, W. B. *Acc. Chem. Res.* **2002**, *35*, 511–522. (e) Moulton, B.; Zaworotko, M. J. *Chem. Rev.* **2001**, *101*, 1629–1658. (f) Goodgame, D. M. L.; Grachvogel, D. A.; Williams, D. J. *Angew. Chem., Int. Ed.* **1999**, *38*, 153–156. (g) Gimeno, N.; Vilar, R. *Coord. Chem. Rev.* **2006**, *250*, 3161–3189. (h) Bauer, C. A.; Timofeeva, T. V.; Settersten, T. B.; Patterson, B. D.; Liu, V. H.; Simmons, B. A.; Allendorf, M. D. *J. Am. Chem. Soc.* **2007**, *129*, 7136–7144. (i) Kaye, S. S.; Long, J. R. *J. Am. Chem. Soc.* **2008**, *130*, 806–807. (j) Cho, S. H.; Ma, B. Q.; Nguyen, S. T.; Hupp, J. T.; Albrecht-Schmitt, T. E. *Chem. Commun.* **2006**, 2563–2565. (k) Horcajada, P.; Surlblé, S.; Serre, C.; Hong, D. Y.; Seo, Y. K.; Chang, J. S.; Grenèche, J. M.; Margiolaki, I.; Férey, G. *Chem. Commun.* **2007**, 2820–2822.
- (2) (a) Kitagawa, S.; Kitaura, R.; Noro, S. *Angew. Chem., Int. Ed.* **2004**, *43*, 2334–2375. (b) Biradha, K.; Sarkar, M.; Rajput, L. *Chem. Commun.* **2006**, 4169–4179. (c) Surlblé, S.; Serre, C.; Mellot-Draznieks, C.; Millange, F.; Férey, G. *Chem. Commun.* **2006**, 284–286. (d) Papaefstathiou, G. S.; MacGillivray, L. R. *Coord. Chem. Rev.* **2003**, *246*, 169–184.
- (3) (a) Rao, C. N. R.; Natarajan, S.; Vaidhyanathan, R. *Angew. Chem., Int. Ed.* **2004**, *43*, 1466–1496. (b) Rosi, N. L.; Kim, J.; Eddaoudi, M.; Chen, B. L.; O'Keeffe, M.; Yaghi, O. M. *J. Am. Chem. Soc.* **2005**, *127*, 1504–1518. (c) Cao, R.; Sun, D. F.; Liang, Y. C.; Hong, M. C.; Tatsumi, K.; Shi, Q. *Inorg. Chem.* **2002**, *41*, 2087–2094.
- (4) (a) Chui, S. S. Y.; Lo, S. M. F.; Charmant, J. P. H.; Orpen, A. G.; Williams, L. D. *Science* **1999**, *283*, 1148–1150. (b) Rowsell, J. L. C.; Yaghi, O. M. *Angew. Chem., Int. Ed.* **2005**, *44*, 4670–4679. (c) Li, H. L.; Eddaoudi, M.; O'Keeffe, M.; Yaghi, O. M. *Nature* **1999**, *402*, 276–279. (d) Rowsell, J. L. C.; Spencer, E. C.; Echert, J.; Howard, J. A. K.; Yaghi, O. M. *Science* **2005**, *309*, 1350–1354.
- (5) (a) Forster, P. M.; Cheetham, A. K. *Angew. Chem., Int. Ed.* **2002**, *41*, 457–459. (b) Vaidhyanathan, R.; Natarajan, S.; Rao, C. N. R. *Inorg. Chem.* **2002**, *41*, 5226–5234. (c) Serpaggi, F.; Luxbacher, T.; Cheetham, A. K.; Férey, G. *J. Solid State Chem.* **1999**, *145*, 580–586. (d) Burrows, A. D.; Harrington, R. W.; Mahon, M. F.; Price, C. F. J. *Chem. Soc., Dalton Trans.* **2000**, 3845–3854.
- (6) (a) Livage, C.; Egger, C.; Noguez, M.; Férey, G. *J. Mater. Chem.* **1998**, *8*, 2743–2747. (b) Livage, C.; Egger, C.; Férey, G. *Chem. Mater.* **1999**, *11*, 1546–1550. (c) Livage, C.; Egger, C. *Chem. Mater.* **2001**, *13*, 410–414. (d) Forster, P. M.; Burbank, A. R.; Livage, C.; Férey, G.; Cheetham, A. K. *Chem. Commun.* **2004**, 368–369. (e) Forster, P. M.; Burbank, A. R.; O'Sullivan, M. C.; Guillou, N.; Livage, C.; Férey, G.; Stock, N.; Cheetham, A. K. *Solid State Sci.* **2005**, *7*, 1549–1555. (f) Livage, C.; Forster, P. M.; Guillou, N.; Tafuya, M. M.; Cheetham, A. K.; Férey, G. *Angew. Chem., Int. Ed.* **2007**, *46*, 5877–5879.
- (7) Lee, E. W.; Kim, Y. J.; Jung, D. Y. *Inorg. Chem.* **2002**, *41*, 501–506.

(8) Boudreaux, E. A.; Mulay, L. N. *Theory and Applications of Molecular Paramagnetism*; John Wiley & Sons: New York, 1976.

Table 1. Summary of Crystal Data, Data Collection, Structure Solution and Refinement Details for **1-7** ($T = 293(2)$)

param	1	2	3	4	5	6	7
empirical formula	C ₅ H ₁₆ CoO ₉	C ₁₀ H ₁₂ CoNa ₂ O ₈	C ₁₅ H ₂₂ Na ₂ O ₁₂	C ₂₀ H ₄₆ Co ₃ O ₂₆	C ₂₀ H ₅₈ Co ₃ O ₃₂	C ₁₅ H ₃₈ Co ₃ O ₂₂	C ₂₀ H ₄₀ Co ₃ Na ₂ O ₂₄
formula mass	279.11	365.11	440.31	879.36	987.45	747.24	887.29
crystal system	orthorhombic	monoclinic	monoclinic	triclinic	triclinic	monoclinic	triclinic
space group	$P2_12_12_1$	$C2/c$	$P2_1/c$	$P\bar{1}$	$P\bar{1}$	$C2/c$	$P\bar{1}$
a (Å)	5.097(3)	17.582(2)	8.145(1)	8.362(2)	8.920(1)	10.099(2)	8.003(2)
b (Å)	11.460(0)	7.672(1)	13.740(2)	9.455(2)	9.492(1)	15.087(2)	9.285(2)
c (Å)	18.100(4)	10.431(1)	17.299(2)	12.628(3)	13.636(2)	18.507(3)	12.436(3)
α (deg)				95.07(3)	81.30(1)		75.96(3)
β (deg)		110.82(8)	94.602(9)	107.35(3)	78.88(1)	104.34(1)	73.45(3)
γ (deg)				113.69(3)	62.21(1)		68.24(3)
volume (Å ³)	1057.3(2)	1315.1(0)	1929.7(4)	847.5(3)	999.7(2)	2731.9(8)	812.9(3)
Z	4	4	4	1	1	4	1
D_{calc} (g cm ⁻³)	1.753	1.844	1.516	1.723	1.640	1.817	1.813
$F(000)$	580	740	920	455	515	1540	455
μ (mm ⁻¹)	1.653	1.407	0.168	1.550	1.334	1.895	1.636
θ range (deg)	2.10–27.49	2.48–27.49	1.90–27.49	3.03–27.48	1.53–27.50	2.27–27.50	1.73–27.50
tot. no. of data colled	1994	1906	5801	7948	5475	3946	4528
no. of obsd data ($I \geq 2\sigma(I)$)	1681	1318	2288	3265	2341	1927	3041
R_1 , wR_2 [$I \geq 2\sigma(I)$] ^a	0.0244, 0.0571	0.0268, 0.0656	0.0443, 0.0981	0.0561, 0.1401	0.0473, 0.0871	0.0557, 0.1079	0.0585, 0.1685
R_1 , wR_2 (all data) ^a	0.0319, 0.0600	0.0332, 0.0688	0.1067, 0.1269	0.0637, 0.1478	0.1176, 0.1180	0.1099, 0.1263	0.0705, 0.1830
Goodness-of-fit on F^2	1.039	1.032	1.001	1.057	0.989	1.025	1.049
no. of variables	167	99	275	226	302	190	224
largest diff peak and hole (e Å ⁻³)	0.284, -0.393	0.336, -0.249	0.337, -0.253	1.683, -0.838	0.705, -0.440	0.433, -0.624	1.148, -1.715

^a $R_1 = \sum(|F_o| - |F_c|)/\sum|F_o|$, $wR_2 = [\sum w(F_o^2 - F_c^2)^2/\sum w(F_o^2)^2]^{1/2}$, and $w = [\sigma^2(F_o^2) + (aP)^2 + bP]^{-1}$ where $P = (F_o^2 + 2F_c^2)/3$. For **1**, $a = 0.0225$ and $b = 0.2989$. For **2**, $a = 0.0267$ and $b = 0.9602$. For **3**, $a = 0.0505$ and $b = 0.0$. For **4**, $a = 0.0796$ and $b = 0.3335$. For **5**, $a = 0.0355$ and $b = 0.0$. For **6**, $a = 0.0511$ and $b = 0.3668$. For **7**, $a = 0.1235$ and $b = 1.1887$.

respective fine glass fibers which were then mounted on a Bruker P4 diffractometer with graphite-monochromated Mo K α radiation ($\lambda = 0.71073$ Å) for cell determination and subsequent data collection. The lattice parameters were refined from the 2θ values (10 – 25°) of 25 carefully centered reflections. The reflection intensities with $2\theta_{\text{max}} = 55^\circ$ were collected at 293 K using the ϑ – 2ϑ scan technique. On the basis of the monitored reflections, the employed single crystals exhibit no detectable decay during the data collection. The data were corrected for L_p and absorption effects. The SHELXS-97 and SHELXL-97 programs^{9,10} were used for structure solution and refinement. The structures were solved by using direct methods. Subsequent difference Fourier syntheses enabled all non-hydrogen atoms to be located. After several cycles of refinement, all hydrogen atoms associated with carbon atoms were geometrically generated, and the rest of the hydrogen atoms were located from the successive difference Fourier syntheses. Finally, all non-hydrogen atoms were refined with anisotropic displacement parameters by the full-matrix least-squares technique and hydrogen atoms with isotropic displacement parameters. For convenience of comparison, the atoms in **4**–**6** are similarly numbered. Detailed information about the crystal data and structure determination is summarized in Table 1. Selected interatomic distances and bond angles are given in Tables S1–S7. Crystallographic data (excluding structure factors) for the structures in this paper have been deposited with Cambridge Crystallographic Data Centre as supplementary publication nos. CCDC 695694 (C₅H₁₆CoO₉), CCDC 695695 (C₁₀H₁₂CoNa₂O₈), CCDC 695696 (C₁₅H₂₂Na₂O₁₂), CCDC 695697 (C₂₀H₄₆Co₃O₂₆), CCDC 695698 (C₂₀H₅₈Co₃O₃₂), CCDC 695699 (C₁₅H₃₈Co₃O₂₂), and CCDC 695700 (C₂₀H₄₀Co₃Na₂O₂₄). Copies of the data can be obtained, free of charge, on application to CCDC, 12 Union Road, Cambridge CB2 1EZ, U.K. (fax +44 1223 336033 or e-mail deposit@ccdc.cam.ac.uk).

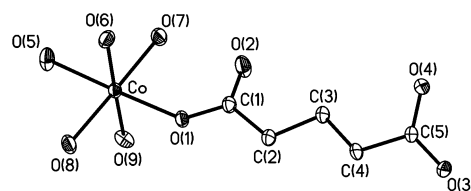


Figure 1. Oak Ridge Thermal Ellipsoid Plot (ORTEP) view of a $[\text{Co}(\text{H}_2\text{O})_5\text{L}]$ complex molecule with displacement ellipsoids (45% probability) and atomic labeling in **1**.

Results and Discussion

Syntheses. Reaction of glutaric acid (C₅H₈O₄), Co(ClO₄)₂·6H₂O and NaOH in an aqueous solution yielded **1**, and **2** was obtained from the hydrothermal self-assembly of Co²⁺ ions and (C₅H₈O₄)²⁻ anions in the presence of 4,4'-bipyridine in an aqueous solution, which was initially aimed at syntheses of mixed ligand complexes of cobalt(II) bipyridine glutarates similar to those previously reported by this laboratory.¹¹ Reaction of CoCl₂·6H₂O, glutaric acid and Na₂CO₃ resulted in a mixture of **4** and **5**, while neutralization of an aqueous solution of CoCl₂·6H₂O and glutaric acid gave a mixture of **6** and **7**.

Description of the Crystal Structures. **Co(H₂O)₅L (1).** Compound **1** crystallizes in a chiral space group $P2_12_12_1$ and the asymmetric unit consists of a Co²⁺ ion, a (C₅H₈O₄)²⁻ anion, and five aqua ligands. The aqua ligand and the monodentate glutarate anion coordinate a Co²⁺ ion to form $[\text{Co}(\text{H}_2\text{O})_5\text{L}]$ complex molecules (Figure 1). To the best of our knowledge, **1** represents a first example of mononuclear α,ω -dicarboxylato complex molecules since α,ω -dicarboxylate anions generally serve as bridging ligands to connect

(9) Sheldrick, G. M. *SHELXS-97, Program for Crystal Structure Solution*; University of Göttingen: Göttingen, Germany, 1997.
 (10) Sheldrick, G. M. *SHELXL-97, Program for Crystal Structure Refinement*; University of Göttingen: Göttingen, Germany, 1997.

(11) (a) Zheng, Y. Q.; Kong, Z. P. *Z. Anorg. Allg. Chem.* **2003**, 629, 1469–1471. (b) Zheng, Y. Q.; Lin, J. L.; Kong, Z. P. *Inorg. Chem.* **2004**, 43, 2590–2596. (c) Zheng, Y. Q.; Ying, E. B. *Polyhedron* **2005**, 24, 397–406.

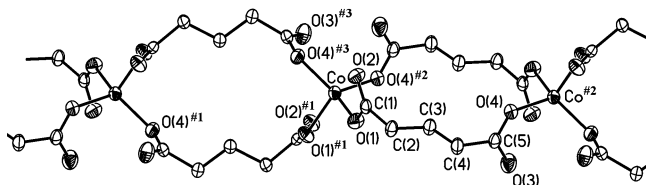


Figure 2. ORTEP view of a fragment of a necklace-like anionic chains ${}^1[\text{CoL}_{42}]^{2-}$ with displacement ellipsoids (45% probability) and atomic labeling in **2**.

metal ions into polymeric architectures.¹² Within the $[\text{Co}(\text{H}_2\text{O})_5\text{L}]$ complex molecule, the Co—O bond distances fall in the region 2.087–2.104 Å, and the cisoid and transoid O—Co—O bond angles in the regions 85.86–92.63° and 176.06–177.61°, respectively, indicating the octahedral coordination to be significantly distorted. The complex molecules display an intramolecular hydrogen bond between an aqua oxygen (O7) to an uncoordinating carboxylato oxygen (O2) with $d(\text{D}\cdots\text{A}) = 2.602$ Å (Table S1). Extensive intermolecular hydrogen bonding interactions are present from the aqua ligands to the carboxylato oxygen atoms except for the aqua O5 ligand, which is found to be hydrogen bonded to an aqua and an uncoordinating carboxylato oxygen atoms of two neighboring complex molecules. Obviously, the intermolecular hydrogen bonds are responsible for the supramolecular assembly of the complex molecules into a 3D supramolecular architecture.

Na₂[CoL₂] (2). The asymmetric unit consists of two halves Na^+ ions, half a Co^{2+} ion, and a glutarate ($\text{C}_5\text{H}_8\text{O}_4$)²⁻ anion, and the Co atoms on the 2-fold axes are each tetrahedrally coordinated by four symmetry-related bisonodentate glutarate anions. The Co—O bond distances are 1.964 and 1.974 Å, respectively, and the O—Co—O bond angles vary from 92.20(8) to 119.06(6)°, being significantly deviated from the value for an ideal tetrahedron. Along [101] direction, the Co^{2+} ions are doubly bridged by glutarate ligands to generate necklace-like chains formulated as ${}^1[\text{CoL}_{42}]^{2-}$ (Figure 2). The resulting anionic chains are arranged according to a pseudo close-packing pattern and held together by Na^+ ions to build up the crystal structure. The two crystallographically different Na^+ ions, namely Na1 and Na2, are located on an inversion center and a 2-fold axis, respectively. The Na1 atoms are each octahedrally coordinated by six carboxylato oxygen atoms belonging to two neighboring chains, whereas the Na2 atoms are each in an octahedral environment defined by six carboxylato oxygen atoms from four adjacent chains. The Na—O contact distances are in the ranges 2.343–2.445 Å and 2.443–2.504 Å for Na1 and Na2, respectively (Table S2). The resulting NaO_6 octahedra are edge-shared to generate one-dimensional (1D) metal oxide chains along [001]. In this sense, the crystal structure of **2** could be visualized as deriving from the anionic chains connected by the metal oxide chains.

Na₂[L(H₂L)_{4/2}] (3). The asymmetric unit of **3** consists of two Na^+ cations, a glutarate ($\text{C}_5\text{H}_6\text{O}_4$)²⁻ anion, and two

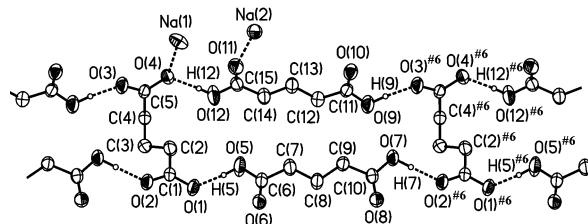


Figure 3. ORTEP view of a fragment of a hydrogen bonded ladder-like anionic chains ${}^1[\text{L}(\text{H}_2\text{L})_{42}]^{2-}$ with displacement ellipsoids (45% probability) and atomic labeling in **3**.

glutaric acid molecules. The two crystallographically distinct dicarboxylic acid molecules exhibit nearly perfect coplanarity of the non-hydrogen atoms. As shown in Figure 3, the glutaric acid molecules extend in the [010] direction. The twisted glutarate anions assume an anti-gauche conformation with a torsion angle of $-58.7(3)^\circ$ for the C2—C3—C4—C5 chain. The oxygen atoms of the glutarate anions are engaged in nearly linear, strong hydrogen bonds to four adjacent glutaric acid molecules with $d(\text{D}\cdots\text{A}) = 2.499$ – 2.566 Å and $\angle(\text{D—H}\cdots\text{A}) = 173$ – 175° (Table S3). The resulting anionic hydrogen bonded ladder-like anionic chains ${}^1[\text{L}(\text{H}_2\text{L})_{42}]^{2-}$ propagate infinitely in the [010] direction. The Na(1) atoms are each pentacoordinated by two carboxylato oxygen atoms of different glutarate anions and three carboxide oxygen atoms of different glutaric acid molecules to form a distorted square pyramidal geometry with $d(\text{Na—O}) = 2.278$ – 2.730 Å, and the Na(2) atoms are in substantially distorted octahedra, each of which is defined by two carboxylato oxygen atoms of different glutarate anions and four carboxide oxygen atoms of different glutaric acid molecules with the Na—O contact distances in the region 2.317– 2.711 Å (Table S3). The anionic chains are held together by Na^+ cations to form two-dimensional (2D) layers parallel to (100), and the resulting layers are stacked to meet the requirement of close-packing. The shortest $\text{Na}\cdots\text{Na}$ separation is 3.497(1) Å.

{[Co₃(H₂O)₆L₂](HL)₂}·4H₂O (4) and {[Co₃(H₂O)₆L₂](HL)₂}·10H₂O (5). Compounds **4** and **5** are composed of the centrosymmetric trinuclear $\{[\text{Co}_3(\text{H}_2\text{O})_6\text{L}_2](\text{HL})_2\}$ complex molecules (Figure 4) and lattice H_2O molecules. They differ from each other in the content of lattice H_2O molecules. For convenience of comparison, the atoms in both compounds are similarly numbered (Figure 4). Within the trinuclear Co(II) complex molecules, three Co(II) atoms are linearly bridged by two symmetry-related glutarate anions through four μ_2 -O atoms. The center Co(1) atom is chelated by two dicarboxylate with the oxygen atoms at the equatorial positions, and the chelating oxygen atoms are additionally bonded to the side Co(2) atoms. Furthermore, a bidentate carboxylate group of a hydrogen glutarate anion bridges the Co(1) and Co(2) atoms, and three aqua ligands coordinate the side Co(2) atom to complete a distorted octahedral coordination geometry (Tables S4 and S5). In comparison with the Co(2) atoms, the center Co(1) atom exhibits a more significantly distorted octahedral coordination according to the cisoid O—Co—O angles (Tables S4 and S5). The Co atoms display usual Co—O bond lengths. From Tables S4

(12) (a) Whelan, E.; Devereux, M.; McCann, M.; McKee, V. *Chem. Commun.* **1997**, 427–428. (b) Zheng, Y. Q.; Sun, J. *J. Solid State Chem.* **2003**, 172, 288–295.

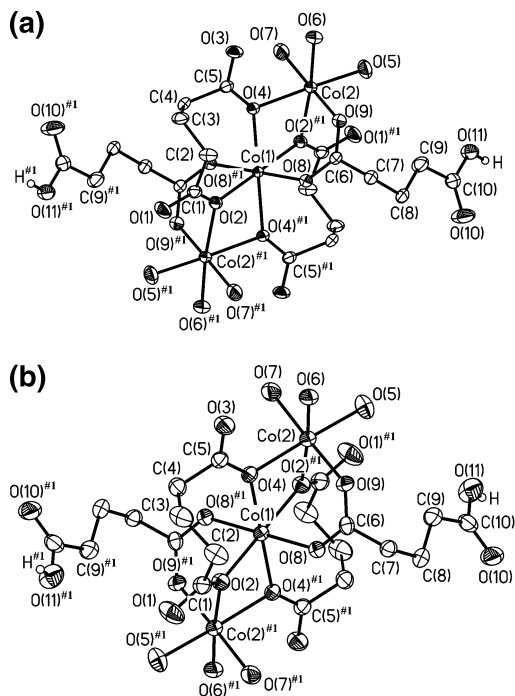


Figure 4. ORTEP view of $[\text{Co}_3(\text{H}_2\text{O})_6\text{L}_2][\text{HL}_2]$ complex molecules with displacement ellipsoids (45% probability) and atomic labeling (a) in **4** and (b) in **5**.

and **S5**, it can be seen that the Co—O contacting interaction is trivially stronger to the hydrogen glutarate anion than to other ligands. The Co—O bonds to the carboxylate oxygen atoms in **4** are slightly longer than the corresponding ones in **5**. The Co(1)···Co(2) separation of 3.262(1) Å in **4** is slightly larger than the value of 3.213(1) Å in **5**. The complex molecules possess intramolecular hydrogen bonds between the aqua ligand and the carboxylate oxygen atoms of glutarate ligands with $d(\text{O}5\cdots\text{O}1^{\#1}) = 2.686$ Å and 2.662 Å for **4** and **5**, respectively, and $d(\text{O}6\cdots\text{O}3) = 2.674$ Å and 2.671 Å for **4** and **5**, respectively. The intermolecular hydrogen bonds from carboxyl group (O11) to non-chelating oxygen atom (O1^{#4}) of the glutarate ligand, as well as those from the aqua ligand (O6) to carboxyl group (O10^{#2}), interlink the complex molecules into 2D networks parallel to (10 $\bar{1}$) in **4** (Figure 5a), while the complex molecules in **5** are assembled via intermolecular hydrogen bonds between carboxyl groups as well as those from aqua ligand (O6) to carboxyl group (O10^{#3}) into supramolecular (4,4) layers parallel to (100) (Figure 5b). In **4**, the lattice water molecules sandwiched between the networks are hydrogen bonded to the carboxylate oxygen atoms of glutarate as well as hydrogen glutarate ligands. As illustrated in Figure 6, four of the five crystallographically distinct lattice H_2O molecules in **5** are hydrogen bonded to one another to form interesting $(\text{H}_2\text{O})_8$ clusters, in which three pairs of H_2O molecules form a chair conformation associated with two H_2O molecules at the trans positions. The extensive hydrogen bonding interactions make a significant contribution to the stabilization of the crystal structure of **5**.

$\{[\text{Co}_3(\text{H}_2\text{O})_6\text{L}_2][\text{L}_{2/2}]\cdot 4\text{H}_2\text{O}\}$ (**6**). The asymmetric unit of **6** consists of one and a half Co^{2+} cations, three aqua ligands, one and half-glutarate anions, and two lattice water mol-

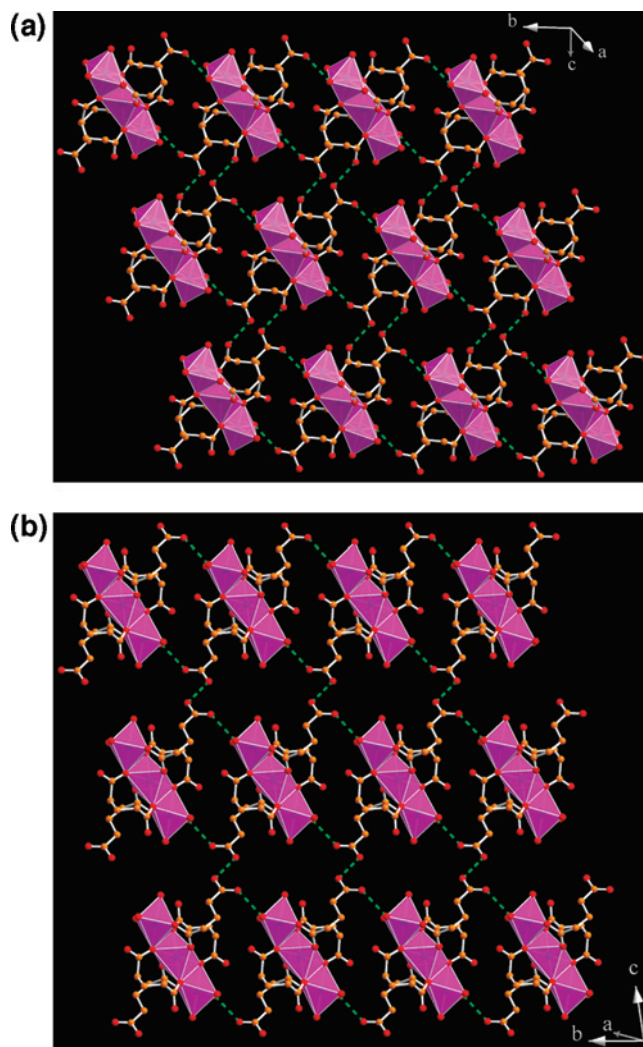


Figure 5. Hydrogen bonded 2D layers resulting from supramolecular assembly of the $[\text{Co}_3(\text{H}_2\text{O})_6\text{L}_2][\text{HL}_2]$ complex molecules (a) in **4** and (b) in **5**.

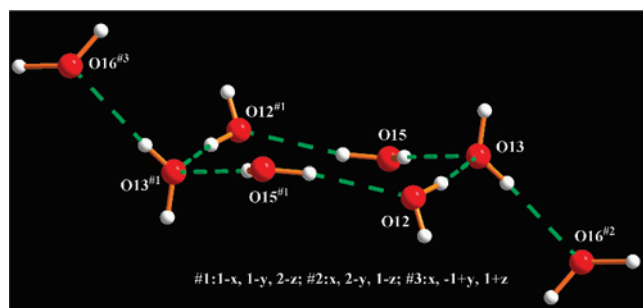


Figure 6. Octameric water $(\text{H}_2\text{O})_8$ cluster in **5**.

ecules. The lattice water molecules are found to be disordered and modeled over two split positions with occupancies in ratio of 0.25:0.75 and 0.4:0.6, respectively, for O10 and O11. The present compounds exhibit the familiar building units of trinuclear Co(II) clusters observed in **4** and **5** except that the partially deprotonated hydrogen glutarato ligands of the complex molecules in **4** and **5** are now replaced by nearly linear bis-bidentate glutarato ligands. As a result, polymeric chains formulated as $\frac{1}{\infty}\{[\text{Co}_3(\text{H}_2\text{O})_6\text{L}_2][\text{L}_{2/2}]\}$ are formed and extend infinitely in the [001] direction (Figure 7a). The

numbering scheme in this compound is similar to those in **4** and **5** for the sake of conveniences. The bonding parameters (Table S6) in the polymeric chains are found to be comparable to the corresponding ones in **4** and **5**. The Co...Co separation in present trinuclear $[\text{Co}_3(\text{H}_2\text{O})_6\text{L}_2]^{2+}$ cores is 3.207 Å very close to 3.213 Å in **5**. The present glutarato bridged chains $^1_{\infty}\{[\text{Co}_3(\text{H}_2\text{O})_6\text{L}_2]\text{L}_{22}\}$ are similar to those found in a Co(II) succinato coordination polymer $\text{Co}(\text{H}_2\text{O})_2(\text{C}_4\text{H}_4\text{O}_4)$ reported by Forster and co-workers.^{6d} Two aqua ligands donate hydrogen atoms to two non-chelating carboxylate oxygen atoms of different twisted glutarato ligands to form intrachain hydrogen bonds (Table S6). The interchain hydrogen bonds from aqua ligands to non-chelating carboxylate oxygen atoms, as well as between aqua ligands, are found to be responsible for the assemblage of the polymeric chains into 2D layers parallel (010) as illustrated in Figure 7b. The layers are stacked along the [010] direction and shifted by $1/2 \bar{a}$ with respect to the neighbors. The lattice H_2O molecules are sandwiched between the resulting supramolecular layers.

Na₂[[Co₃(H₂O)₂]L_{8/2}]·6H₂O (7). The asymmetric unit of **7** comprises a Na⁺ cation, one and half Co²⁺ cations, two glutarate anions, one aqua ligand, and three lattice H₂O molecules. Two crystallographically distinct glutarate anions function as bridging ligands in a $\mu_4\text{-}\eta^2\eta^2$ fashion and a $\mu_3\text{-}\eta^1\eta^2$ fashion, respectively. Compound **7** features linear trinuclear (Co₃) cores of corner-shared trioctahedra different from **4–6**, where the linear trinuclear (Co₃) cores exhibit edge-shared trioctahedra. As depicted in Figure 8a, the side

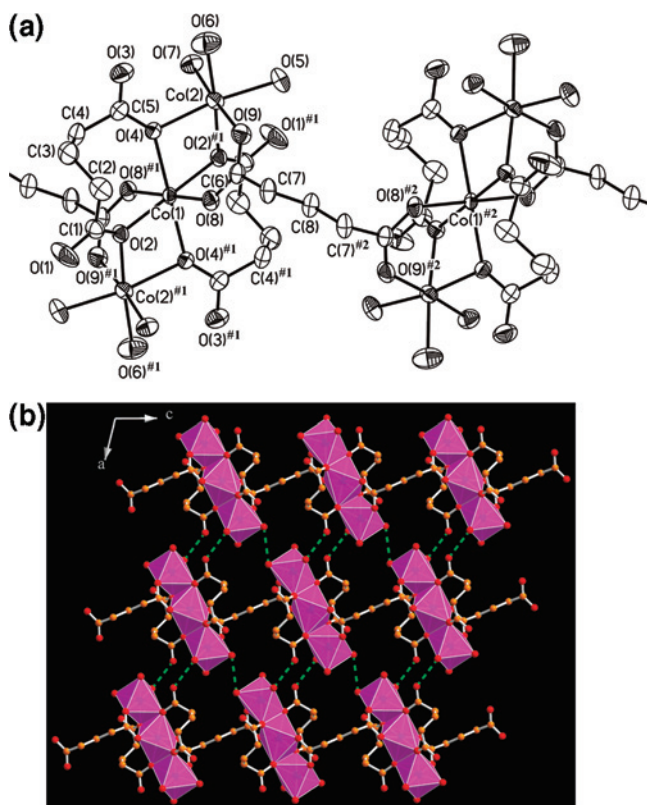


Figure 7. (a) ORTEP view of a fragment of the 1D polymeric chains $^1_{\infty}\{[\text{Co}_3(\text{H}_2\text{O})_6\text{L}_2]\text{L}_{22}\}$ with displacement ellipsoids (45% probability) and atomic labeling in **6**. (b) Supramolecular assembly of the 1D polymeric chains into 2D layers on the basis of interchain hydrogen bonds in **6**.

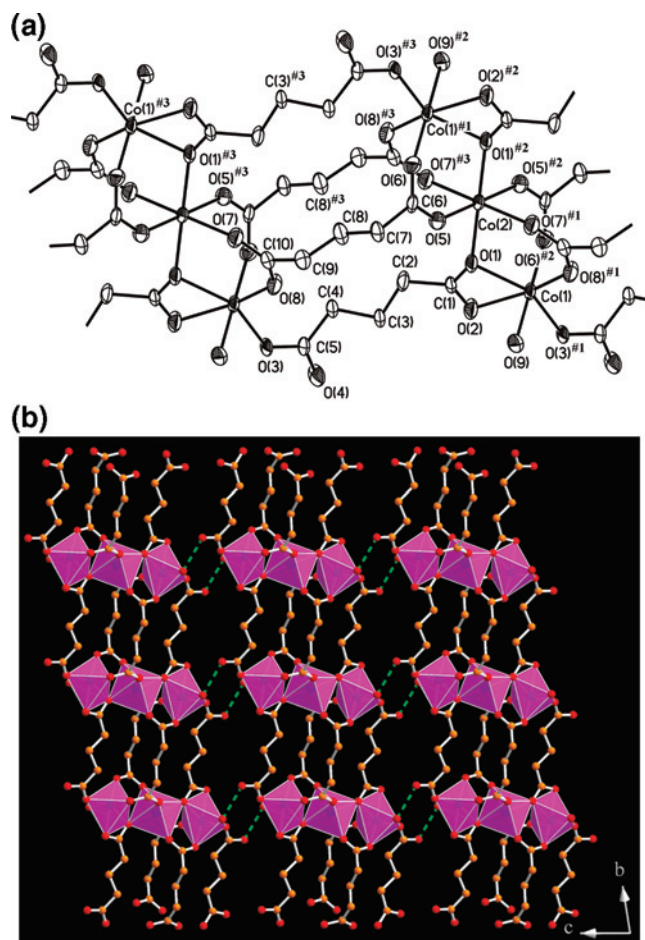


Figure 8. (a) ORTEP view of a fragment of the 1D polymeric chains $^1_{\infty}\{[\text{Co}_3(\text{H}_2\text{O})_2]\text{L}_{8/2}\}^{2-\infty}\{[\text{Co}_3(\text{H}_2\text{O})_2]\text{L}_{8/2}\}^{2-}$ with displacement ellipsoids (45% probability) and atomic labeling in **7**. (b) Supramolecular assembly of the 1D polymeric chains into 2D layers on the basis of interchain hydrogen bonds in **7**.

Co(1) atoms in the present trinuclear (Co₃) cores are each coordinated by six oxygen atoms of one aqua ligand and four carboxylate groups of different glutarato ligands, while the central Co(2) atoms at the inversion center of symmetry are each coordinated by six carboxylate oxygen atoms of different dicarboxylate ligands. The Co...Co separation of 3.535 Å in the present trinuclear [Co₃] cores is substantially larger than those observed in **4–6**. The trinuclear (Co₃) cores are bridged by dicarboxylate ligands to generate anionic chains propagating in [010] directions (Figure 8a). The chains could be viewed as resulting from incorporation of a glutarate anion into the neutral polymeric $^1_{\infty}\{[\text{Co}_3(\text{H}_2\text{O})_6\text{L}_2]\text{L}_{22}\}$ chains in **6**. The present anionic chains are supramolecularly assembled via interchain hydrogen bonds from aqua ligand to non-coordinating carboxylate oxygen atom into 2D layers parallel to (100) as shown in Figure 8b. Between the layers are sandwiched the Na⁺ cations and lattice H₂O molecules forming nearly linear hydrogen bonded (H₂O)₃ trimers, which serve as a hydrogen bond acceptor from the aqua ligand and as hydrogen bond donor to the carboxylate oxygen atoms (Table S7). The Na⁺ cations are each distorted octahedrally coordinated by six oxygen atoms from three carboxylate groups, one aqua ligand and two

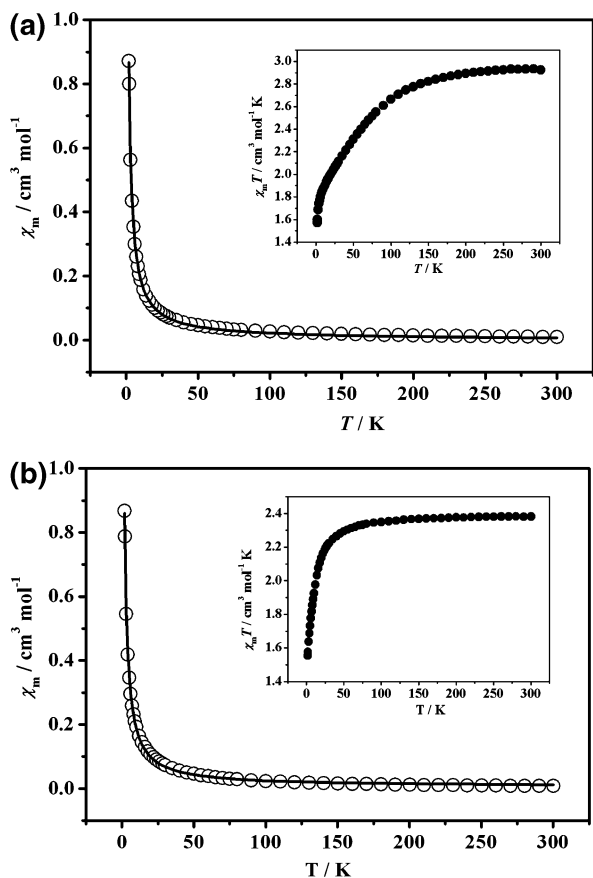


Figure 9. Temperature dependence of the magnetic susceptibilities of (a) **1** and (b) **2** (χ_m being the magnetic susceptibility per Co(II) ion). Solid lines represent the best fits.

lattice H₂O molecules with Na–O contacting distances in the region 2.279–2.702 Å comparable to those observed in **2** and **3**.

Magnetic Properties. We have attempted to investigate the magnetic behavior of this family of cobalt glutarate compounds through variable-temperature magnetic susceptibility measurements. Because of the extremely low yields and difficulty to separate **4–7** from the mixture in a sufficient quantity, magnetic characterizations on **4–7** could not be carried out. Temperature-dependent magnetic susceptibility measurements for compounds **1** and **2** were performed on the polycrystalline sample in the temperature range of 2–300 K in a fixed magnetic field 2 KG, and the magnetic behaviors in the form of χ_m and $\chi_m T$ products versus T plots are depicted in Figure 9 (χ_m being the magnetic susceptibility per a Co(II) ion).

Concerning the compound **1**, the effective magnetic moment at room temperature is 4.84 μ_B , which falls into a reasonable range for complexes containing octahedrally coordinated Co(II) centers in the high-spin state, and the $\chi_m T$ value is 2.93 $\text{cm}^3 \cdot \text{K} \cdot \text{mol}^{-1}$ at room temperature, which is much larger than the spin-only value of 1.87 $\text{cm}^3 \cdot \text{K} \cdot \text{mol}^{-1}$ for high-spin Co(II) ($S = 3/2$). The magnetic behavior should be due to a larger orbital contribution arising from the $^4T_{1g}$ ground state of Co(II). Upon cooling, the $\chi_m T$ value gradually decreases to 1.57 $\text{cm}^3 \cdot \text{K} \cdot \text{mol}^{-1}$ at 2 K. The χ_m can be fit to the Curie–Weiss equation $\chi_m = C/(T - \Theta)$ with the Curie constant $C = 3.012(8) \text{ cm}^3 \cdot \text{mol}^{-1} \cdot \text{K}$ and Weiss constant Θ

$= -9.4(7) \text{ K}$, indicating slight anti ferromagnetic interactions between Co(II) ions. Because high-spin octahedral Co(II) (d^7 , $S = 3/2$) has a $^4T_{1g}$ ground state, a detailed quantitative analysis of the susceptibility data is complicated by the fact that single-ion effects, such as the orbital moment, spin–orbit coupling, distortions from regular stereochemistry, electron delocalization, and crystal field mixing of excited states into the ground state. When taking into consideration the mono-nuclear Co(II) complex with spin–orbit coupling parameter ($H = \lambda LS$) and parameter A , which gives the measurement of the crystal field strength to the interelectronic repulsions ($x = \lambda/k_B T$), the experimental data were fitted to the equation as follows¹³

$$\chi_{\text{momo}} = \frac{N\beta^2}{3kT} \left\{ \frac{7(3-A)^2x}{5} + \frac{12(A+2)^2}{25A} + \left[\frac{2(11-2A)^2x}{45} + \frac{176(A+2)^2}{675A} \right] \exp\left(-\frac{5Ax}{2}\right) + \left[\frac{(A+5)^2x}{9} - \frac{20(A+2)^2}{27A} \right] \times \exp(-4Ax) \right\} / \left\{ \frac{x}{3} \left[3 + 2 \exp\left(-\frac{5Ax}{2}\right) + \exp(-4Ax) \right] \right\} \quad (1)$$

where A is a crystal field parameter ($A = 1.5$ is the weak-field limit, $A = 1.32$ is for a free ion, and $A = 1.0$ is the strong-field limit), λ is the spin–orbit coupling constant ($\lambda = -176.0 \text{ cm}^{-1}$ is the free-ion value), k_B represents the electron delocalization ($k_B = 1.0$ is minimal).¹⁴ Because of the very weak magnetic interactions between ions, the expression in eq 1 was corrected using the molecular field approximation (eq 2), to which the present measured magnetic susceptibility data were fitted,

$$\chi_m = \frac{\chi_{\text{momo}}}{1 - (2zJ/Ng^2\beta^2)\chi_{\text{momo}}} \quad (2)$$

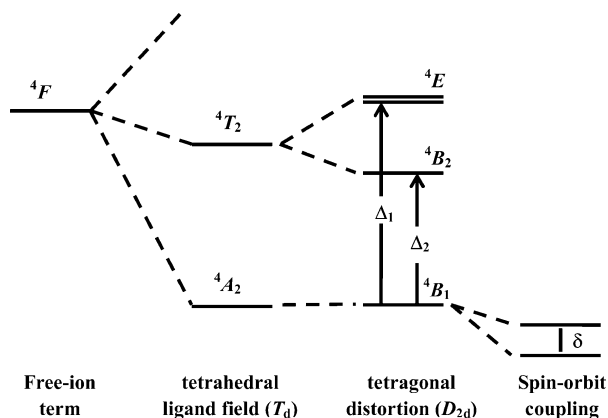
where χ_m is the exchange coupled magnetic susceptibility actually measured, χ_{momo} is also the magnetic susceptibility in the absence of the exchange field, zJ is the total exchange parameter between Co(II) ions, and the rest of the parameters have their usual meanings. The best fit is obtained with values of $g = 2.18$, $\lambda = -117 \text{ cm}^{-1}$, $A = 1.5$, $zJ = -0.08 \text{ cm}^{-1}$, and the agreement factor R is 8.5×10^{-6} ($R = \sum[(\chi_m)_{\text{obs}} - (\chi_m)_{\text{calc}}]^2 / [(\chi_m)_{\text{obs}}]^2$). The fitting results indicate that the surrounding of Co(II) is the comparatively strong-field state and a slightly distorted octahedral arrangement which is consistent with the crystal structure.

At room temperature, the effective magnetic moment of compound **2** is 4.37 μ_B , and the $\chi_m T$ value is 2.38 $\text{cm}^3 \cdot \text{K} \cdot \text{mol}^{-1}$, which is much larger than the spin-only value of 1.87 $\text{cm}^3 \cdot \text{K} \cdot \text{mol}^{-1}$ for high-spin Co(II) ($S = 3/2$) but they are common values for high-spin complexes in tetrahedral Co(II) centers (4.30–5.20 μ_B). The magnetic behavior should be due to a larger orbital contribution arising from the $^4A_{2g}$ ground-state of Co(II). Upon cooling, the $\chi_m T$ value remains nearly constant up to 50 K, then abruptly diminishes to 1.56 $\text{cm}^3 \cdot \text{K} \cdot \text{mol}^{-1}$ at 2 K, which is typical of an overall antiferromagnetic interaction between Co(II) ions. The χ_m

(13) Mabbs, F. E.; Machin, D. J. *Magnetism and Transition Metal Complexes*; Chapman and Hall: London, 1973; pp 99–100.

(14) Raebiger, J. W.; Manson, J. L.; Sommer, R. D.; Geiser, U.; Rheingold, A. L.; Miller, J. S. *Inorg. Chem.* **2001**, *40*, 2578–2581.

Scheme 1



can be fit to the Curie–Weiss equation $\chi_m = C/(T - \Theta)$ with the Curie constant $C = 2.40(1) \text{ cm}^3 \cdot \text{mol}^{-1} \cdot \text{K}$ and the Weiss constant $\Theta = -2.10(5) \text{ K}$. The partial splitting diagram of the 4F term for a free Co(II) ion under the action of a tetragonally distorted tetrahedral crystal field and spin–orbit coupling is illustrated in Scheme 1, and a magnetic susceptibility equation was obtained as follows¹⁵

$$\chi_{\text{mono}} = \frac{N\beta^2}{3kT} \left[5x^2 + 10y^2 + \frac{2\delta}{kT}(x^2 - y^2) \right] + \frac{8N\beta^2\kappa^2}{3} \left[\frac{2}{\Delta_1} + \frac{1}{\Delta_2} \right] \quad (3)$$

where $x = (1 - 4\kappa\lambda/\Delta_1)$, $y = (1 - 4\kappa\lambda/\Delta_2)$, λ is the spin–orbit coupling constant ($\lambda = -176.0 \text{ cm}^{-1}$ is the free-ion value), κ represents a reduction in the orbital angular momentum, and δ , Δ_1 , and Δ_2 are defined in Scheme 1. The expression (eq 1) must also be corrected for the magnetic exchange because of very weak magnetic interactions between ions, and the molecular field approximation was employed for this purpose and is illustrated in eq 3,

$$\chi_m = \frac{\chi_{\text{mono}}}{1 - (2zJ/Ng^2\beta^2)\chi_{\text{mono}}} \quad (4)$$

where χ_m is the exchange coupled magnetic susceptibility actually measured, χ_{mono} is also the magnetic susceptibility

(15) Mabbs, F. E.; Machin, D. J. *Magnetism and Transition Metal Complexes*; Chapman and Hall: London, 1973; pp 143–149.

in the absence of the exchange field, zJ is the exchange parameter, and the rest of the parameters have their usual meanings. The best fit is obtained with values of $g = 2.10$, $\lambda = -110 \text{ cm}^{-1}$, $\kappa = 1.0$, $\delta = 20 \text{ cm}^{-1}$, $\Delta_1 = 3600 \text{ cm}^{-1}$, $\Delta_2 = 3000 \text{ cm}^{-1}$, $zJ = -0.05 \text{ cm}^{-1}$, and the agreement factor R is 3.3×10^{-4} ($R = \sum[(\chi_m)^{\text{obs}} - (\chi_m)^{\text{calc}}]^2 / [(\chi_m)^{\text{obs}}]^2$).

Conclusion

Self-assembly of Co^{2+} ions and $(\text{C}_5\text{H}_8\text{O}_4)^{2-}$ anions in the presence of NaOH or Na_2CO_3 under ambient or hydrothermal conditions yielded a series of new glutarate cobalt coordination polymers $\text{Co}(\text{H}_2\text{O})_5\text{L}$ **1**, $\text{Na}_2[\text{CoL}_2]$ **2**, $\text{Na}_2[\text{L}(\text{H}_2\text{L})_{4/2}]$ **3**, $\{[\text{Co}_3(\text{H}_2\text{O})_6\text{L}_2](\text{HL})_2\} \cdot 4\text{H}_2\text{O}$ **4**, $\{[\text{Co}_3(\text{H}_2\text{O})_6\text{L}_2](\text{HL})_2\} \cdot 10\text{H}_2\text{O}$ **5**, $\{[\text{Co}_3(\text{H}_2\text{O})_6\text{L}_2]\text{L}_{2/2}\} \cdot 4\text{H}_2\text{O}$ **6**, and $\text{Na}_2\{[\text{Co}_3(\text{H}_2\text{O})_2]\text{L}_{8/2}\} \cdot 6\text{H}_2\text{O}$ **7**, and the intriguing building units are the linear edge-shared trioctahedral Co_3O_{14} chromophores in **4**, **5**, and **6** and corner-shared trioctahedral Co_3O_{16} chromophores in **7**. Complexes **1** and **2** display magnetic behaviors following the Curie–Weiss law $\chi_m = C/(T - \Theta)$ with the Curie constant $C = 3.012(8) \text{ cm}^3 \cdot \text{mol}^{-1} \cdot \text{K}$ and Weiss constant $\Theta = -9.4(7) \text{ K}$ for **1**, as well as $C = 2.40(1) \text{ cm}^3 \cdot \text{mol}^{-1} \cdot \text{K}$ and $\Theta = -2.10(5) \text{ K}$ for **2**, indicating weak antiferromagnetic interactions between Co(II) ions, and the best-fitting of the magnetic susceptibility of **2** afforded some important splitting parameters for tetrahedrally coordinated Co(II) ion under the action of a tetragonally distorted tetrahedral crystal field and spin–orbit coupling.

Acknowledgment. This project was sponsored by the K. C. Wong Magna Fund in Ningbo University and supported by the Expert Project of Key Basic Research of the Ministry of Science and Technology of China (Grant 2003CCA00800), the Zhejiang Provincial Natural Science Foundation (Grant Z203067), and the Ningbo Municipal Natural Science Foundation (Grant 2006A610061).

Supporting Information Available: Selected interatomic distances and bond angles for **1–7**. X-ray crystallographic CIF files for all compounds in this work. This material is available free of charge via the Internet at <http://pubs.acs.org>.

IC801053P